Mechanism of Amine Sensitization in Shocked Nitromethane

Yuri A. Gruzdkov* and Yogendra M. Gupta†

Institute for Shock Physics and Department of Physics, Washington State University, Pullman, Washington 99164-2814

Received: November 25, 1997

The mechanism of amine sensitization of shocked nitromethane was investigated using time-resolved optical absorption spectroscopy in the visible. Neat nitromethane and mixtures of nitromethane with six different (primary, secondary, tertiary, and di-) amines were shocked to within 12−17 GPa peak pressure using step wave loading. Despite the small amine concentrations, profound differences were observed in the absorption spectra of neat and sensitized nitromethane. The changes in the absorption spectrum of reacting neat nitromethane consisted of irreversible broad-band (450−650 nm) loss of transmission through the sample after a short induction time. In contrast, a transient absorption peak at 525 nm developed in the spectra of the reacting mixtures. This feature did not depend on the particular amine used. We assign it to a transient intermediate formed in the shocked mixtures during the early stages of decomposition. On the basis of our analyses and the data available in the literature, we identify the intermediate as a radical anion of nitromethane, $CH_3NO_2^{\bullet-}$. The implications of this on the mechanism of sensitization are discussed. Several possible radical anion mechanisms are considered and evaluated. The base catalysis by amines is favored as the most plausible mechanism of sensitization. This mechanism is discussed in detail.

I. Introduction

The understanding of shock-induced chemical decomposition is important to the development of new energetic materials, studies of shock initiation and buildup to detonation, impact sensitivity, and explosives safety. The combination of continuum measurements (pressure, particle velocity) and time-resolved spectroscopic techniques is needed to provide the necessary macroscopic and microscopic insight into this challenging problem. While continuum measurements on a number of energetic materials under shock compression have been carried out for a long time,[1] real time optical spectroscopic methods are more recent.[2] In this work, we utilize recent developments in time-resolved spectroscopy (particularly absorption measurements) to examine molecular mechanisms governing shock-induced decomposition of nitromethane.

Nitromethane (NM) is an insensitive high explosive that serves as a good prototypical energetic material; the simplicity of its chemical structure makes it attractive for mechanistic studies. It is also the simplest member of the family of nitro compounds that includes nitroglycerin and trinitrotoluene. Furthermore, it is a liquid and, therefore, many complexities associated with solid materials can be avoided. For these reasons, NM is a very well-studied material; good reviews regarding earlier work on NM may be seen in refs 3 and 4. Thus, information can be drawn from a large body of scientific literature which includes spectroscopic data at ambient pressure,[4] static high-pressure data,[5] and continuum[6] and spectroscopic[7−11] data under shock loading.

It has been known since the late 1940s that NM can be sensitized toward detonation by the addition of small amounts of amines.[12] Quantitative measures of the degree of sensitization came from failure diameter measurements and gap tests.[13−17] Differential scanning calorimetry was used to evaluate the influence of amines on slow thermal decomposition of NM.[4,18] The mechanism of amine sensitization, although widely believed to be chemical in nature, is not well understood. The different hypotheses of sensitization will be reviewed briefly in the next section. There is no agreement between these hypotheses. The objective of this work was to clarify the mechanism of sensitization by following in real time the molecular changes in shocked NM with time-resolved spectroscopic methods.

The previous spectroscopic work on shocked NM utilized Raman and UV−vis absorption (250−450 nm) spectroscopies[7−11] because of their sensitivity to changes in the bulk material. The initiation of chemical reaction is characterized by a small extent of reaction, and therefore, it requires a technique specifically sensitive to reaction intermediates and insensitive to changes in the bulk material. Optical absorption spectroscopy further out in the visible can be used for this purpose because unreacted NM has no appreciable absorption at wavelengths longer than 400 nm at both ambient and high pressure.[7,10] In this work, we extended the accessible wavelengths up to 650 nm. This permitted detection of transient intermediates formed during the decomposition process in shocked NM−amine mixtures and, consequently, delineation of the sensitization mechanism.

Background relevant to this work is in the next section. Section III summarizes the experimental methods; the results are presented in section IV. Section V presents a discussion of our results including assignment of the transient absorption spectra to the intermediate, analysis of reaction kinetics under shock conditions, and the mechanism of sensitization. The main findings are summarized in section VI.

II. Background

A. Absorption Spectra. Time-resolved changes in the visible absorption spectra (400−650 nm) of shocked NM and the NM−amine mixtures are of primary interest. The UV−vis

† Electronic mail: gruzdkov@mail.wsu.edu; ymgupta@wsu.edu.

S1089-5639(98)00323-5 CCC: $15.00
Published on Web 02/26/1998

absorption spectrum of neat NM, at ambient conditions, consists of two broad bands. The longer wavelength band at about 270 nm ($\epsilon \sim 20\ M^{-1}\ cm^{-1}$) is assigned to the n$-\pi^*$ transition; [19−21] the tail of this band extends up to 380 nm. At shock pressures of interest for our work, this tail shifts toward longer wavelengths.[7] The shorter wavelength band centered at around 200 nm ($\epsilon \sim 5000\ M^{-1}\ cm^{-1}$)[19−21] is assigned to the $\pi-\pi^*$ transition and is not observable in our experiments.

The absorption spectrum of the NM−amine mixtures, at ambient conditions, shows a new broad absorption band absent in the absorption spectra of the individual components.[4,18] The position of this band depends on the amine and displays good linear correlation with the ionization energy of the particular amine.[4] Because this relationship is typical for organic charge-transfer complexes,[22] it was interpreted as evidence for the same in the NM−amine mixtures.[4,18] The new absorption band of the complex would originate in the electronic transition from the highest occupied molecular orbital of the amine (the lone electron pair on the nitrogen) to the lowest unoccupied molecular orbital of NM (the NO_2 π^* orbital).[4,18] This band, however, is too weak (for example ca. 2 $M^{-1}\ cm^{-1}$ for ethylenediamine) for detection in our experimental configuration.

B. Nitromethane−Amine Interactions. NM is considered a weak acid ($pK_a = 10.21$).[23] The liquid is, therefore, in equilibrium with the aci-anion and the nitronic acid (or aci-NM):

$$CH_3NO_2 \rightleftharpoons [CH_2NO_2]^- + H^+ \rightleftharpoons CH_2NO_2H \qquad (1)$$

Upon addition of amines (organic bases), NM is expected to undergo an acid−base reaction:

$$CH_3NO_2 + RNH_2 \rightleftharpoons [CH_2NO_2]^- + RNH_3^+ \qquad (2)$$

As mentioned earlier, another plausible form of NM−amine interaction is the formation of molecular (or charge-transfer) complexes. The complex is formed via attraction between the nitro group of NM and amine.[4] Additionally, because NM has a smaller dielectric constant than water, there is an effect of ion pairing.[24]

Effects of high pressure and temperature on equilibria (1) and (2) and the molecular complex are not well established. Some work has been carried out on the effects of static high pressure on neat NM.[25,26] The increased concentration of the aci-anion induced by static high pressure was inferred from hydrogen/deuterium isotope exchange between CH_3NO_2 and CD_3NO_2.[25] It was also calculated, by combining space-filling models with a rough two-level statistical mechanical model of the aci-anion/proton system, that at 5 GPa and 400 K there will be about 80 times more aci-anions present than at ambient conditions.[26]

C. Sensitization of Nitromethane by Amines. Several molecular mechanisms have been put forward to explain the sensitization of NM. The first explanation was proposed by Engelke et al.[26] They suggested that the aci-anion of NM is somehow involved in the rate-determining step. Since the amine addition will increase the aci-anion concentration via reaction 2, it should lead to sensitization. To support this idea, they argued that other factors known to sensitize NM, such as the addition of organic bases, UV irradiation, and static high pressure, provide higher levels of the aci-anion as well.[5,13,14,25−28]

The aci-anion hypothesis has been questioned by some[18,29] for the following reasons. First, it did not offer a specific mechanism. Second, Engelke et al. relied heavily on the NMR data to suggest that the aci-anion of nitromethane was the only new chemical species generated in NM by the sensitizers.[14,25,27] Because of the intrinsically low sensitivity of NMR spectroscopy, other species formed in nitromethane may not be detectable by NMR. Consequently, charge-transfer and hydrogen-bonded complexes were proposed by others as alternatives to the aci-anion hypothesis.[18,29] Finally, there was no concrete evidence that the aci-anions were more reactive than the parent molecules.[18]

Politzer et al.[30] pursued the aci-anion hypothesis further. Using density functional calculations, they found that, of the various possibilities examined, the most energetically favorable reaction is the one involving the aci-anion and amine:

$$[CH_2NO_2]^- + NH_3 \rightarrow CH_3NH_2 + NO_2^- \qquad (3)$$

The key features of this process were emphasized to be[30] an activation barrier less than the C−NO_2 dissociation energy of NM, a net release of energy, and a formation of another amine that can sustain the reaction.

Cook and Haskins[29] have questioned the importance of the aci-anion for sensitization. On the basis of their own calculations, they proposed that NM formed a hydrogen-bonded complex with amines, causing a decrease in the C−N bond dissociation energy of NM. Depending on the geometry of the complex, either of the following reactions was proposed:[29]

$$NH_3 + CH_3NO_2 \rightarrow CH_3NH_3^+ + NO_2^- \qquad (4)$$

$$NH_3 + CH_3NO_2 \rightarrow CH_3NH_2 + HONO \qquad (5)$$

Politzer et al.[30] analyzed reactions 4 and 5. They did find the complexes proposed by Cook and Haskins to be weakly stable. However, they did not find a reduction in both homolytic and heterolytic C−N bond dissociation energy in the complexes compared to NM.

On the basis of slow thermal decomposition measurements, Constantinou et al.[4,18] proposed that sensitization is due to a weakening of the C−N bond of NM, but not through hydrogen bonding. They suggested that a charge-transfer complex, discussed earlier, was responsible for it. The decomposition of charge-transfer complexes was thought to give rise to the initial stage in the thermal decomposition observed for the NM−amine mixtures. This extra stage was interpreted as an indication of a new reaction pathway. It was shown also that the mixtures decompose through a process that follows first-order kinetics while neat NM decomposes through a cubic autocatalytic process.

As seen from the above summary, there is no agreement on the molecular mechanism of amine sensitization. Clearly, experimental data at the molecular level are necessary to address this issue. Ideally, the detection and identification of transient intermediates would help in determining the mechanism of sensitization. Hence, we undertook time-resolved optical absorption experiments in shocked NM−amine mixtures.

III. Experimental Method

The experimental methods were very similar to those used previously, and more details can be seen elsewhere.[7,8,10,11]

A. Materials. All the samples used in this work consisted of neat NM or NM−amine mixtures. Spectrophotometric grade NM (99+% purity) was obtained from Aldrich Chemical Co. The following amines were used: ethylenediamine (EDA), 99+% or 99.5+%; *n*-butylamine (BA), 99+%; diethylamine (DEA), 99.5%; triethylamine (TEA), 99+%; *N*-methylaniline

TABLE 1: List of Experiments

expt no.	sample	cell thickness (μm)	initial temp (K)	projectile velocity (km/s)	shock-up time[a] (ns)	calc press. (GPa)	calc temp (K)
A1 (95-034)	NM	251	323	0.931	130	17.2	991
A2 (95-031)	NM + EDA (37.5 mM)	282	ambient	0.535	350	12.1	734
A3 (95-029)	NM + EDA (18.8 mM)	277	ambient	0.617	310	14.0	767
A4 (95-028)	NM + EDA (18.8 mM)	257	ambient	0.543	310	12.2	737
A5 (96-001)	NM + EDA (75.0 mM)	160	ambient	0.535	200	12.1	734
A6 (96-006)	NM + BA (37.5 mM)	165	ambient	0.529	210	11.9	732
A7 (96-020)	NM + DEA (37.5 mM)	147	ambient	0.527	185	11.9	731
A8 (96-024)	NM + MPA (38.0 mM)	155	ambient	0.523	195	11.8	729
A9 (96-021)	NM + TEA (37.5 mM)	168	ambient	0.526	210	11.8	730
A10 (96-025)	NM + DABCO (36.8 mM)	163	ambient	0.526	210	11.8	730

[a] Time to reach 95% of the final pressure.

(or methylphenylamine, MPA), 99+%; 1,4-diazabicyclo[2.2.2]-octane (DABCO, or triethylenediamine), 98%; all from Aldrich Chemical Co. All the chemicals were used as received, except for EDA (99+%) which was redistilled in the laboratory before use. The NM−amine mixtures were prepared in air 2−5 h before each experiment.

B. Impact Experiments. Shock waves were generated by impacting a sapphire crystal, mounted on a projectile, onto the sapphire front window of the sample cell. The description of cell design can be seen elsewhere.[7,31] The projectile could be accelerated to any velocity up to 1.2 km/s using a single-stage gas gun.[32] After impact it takes approximately 280 ns for a shock wave to traverse the front window and enter the sample. It subsequently reverberates between the front and back sapphire windows until the sample reaches final pressure in several steps. The time required for this process depends on the sample thickness while the final pressure is determined only by the projectile velocity and the sapphire response.[33] During reverberation of the shock wave, the sample temperature also increases in a stepwise fashion. Final pressure is maintained in the sample until release waves come in from the edges of the sapphire windows. Because the data were obtained only from the central 4 mm, the sample was in a state of uniaxial strain for approximately 1 μs after the shock wave entered the sample. In Table 1 we list the parameters for each experiment.

In one experiment (experiment A1, see Table 1) we used a LiF front window instead of sapphire to avoid exceeding the elastic limit of sapphire under shock compression (between 14 and 17 GPa). Because LiF has a lower shock impedance than sapphire, the final pressure in the liquid sample can reach 20 GPa without exceeding the Hugoniot elastic limit of the sapphire impactor.[3] Some minor changes were made to the cell design accordingly. In this experiment we also heated the sample up to 323 K with a heater coil inserted into the brass cell body. Details of experiments with LiF front windows and heater coils can be found elsewhere.[3]

Pressure and temperature histories in the sample, for each experiment, were calculated using the SHOCKUP program.[34] The calculations used a material model describing the shock response of sapphire,[35] LiF, [36] and the equation of state for NM developed in our laboratory.[3] Because the impact velocity and the shock response of the impactor and cell windows are well-known, the calculated final pressures were accurate to within 1−2%. Recent temperature measurements in shocked neat NM, using Raman scattering, showed that the calculated temperature is accurate to at least within ±10%.[37]

C. Time-Resolved Optical Absorption Measurements. A pulsed xenon flashlamp (Xenon Corp., model 457) was used as the light source. The output was filtered with a set of light balancing filters (LA-120, LA-100; Hoya Optics), collimated, and directed into the sample through an aperture 4 mm in diameter. The transmitted light was collected into an optical fiber bundle.[7] Part of it was delivered to the input slit of a grating spectrometer (Spex 1681) coupled to an electronic streak camera (Cordin, model 58), and part of it was delivered to a photomultiplier tube. The photomultiplier tube data served as a diagnostic in these experiments. The spectrometer dispersed the light in wavelength, and the streak camera dispersed it in time. The streak camera output (intensity vs time vs wavelength) was recorded by a CCD detector (Spex CCD 1024 × 256 in experiments A1−A6 and Princeton Instruments TE/CCD-512-TKBM/1 in experiments A7−A10) and digitally displayed as a series of transmission spectra separated by ca. 50 ns time intervals. There was sufficient transmitted light intensity for measurements within 420−650 nm spectral and −0.3 to +1.2 optical density range. Transmission spectra were converted to absorption data as described in ref 7.

IV. Results

A. Neat Nitromethane. Shock-induced decomposition in neat NM has been studied previously with optical absorption spectroscopy.[7,10] Briefly, no evidence for a chemical reaction was found for pressures up to 14 GPa with an initial temperature of 298 K.[7] In experiments with a peak pressure of 17 GPa or above, reaction in NM was observed.[10] It manifested itself in irreversible broad-band loss of transmission through the sample after a short induction time. For all these experiments the data were limited to wavelengths of 500 nm or less.

Experiment A1 was aimed to extend the spectral range up to 650 nm and to attempt detection of the intermediates in *reacting* NM. The parameters of this experiment are given in Table 1. The results are shown in Figure 1. As can be seen, a broad-band loss of transmission eventually occurred similar to that reported by Winey and Gupta.[10] The spectra are essentially featureless. They show a flat absorbance that begins to grow after an induction period of ca. 300 ns. It turns into nearly complete cutoff of light (absorbance greater than 1) after ca. 450 ns.

B. Nitromethane−Ethylenediamine Mixture at 12 GPa. Unlike neat NM, sensitized NM shows signs of chemical reaction at pressures as low as 10 GPa; a precise lower limit was not established.[7] Absorption spectra of the NM−EDA mixture shocked to 12.1 GPa (experiment A2) are shown in Figure 2. As can be seen, after the shock enters the sample an absorption band at 525 nm begins to grow. It continues to grow after the final pressure is reached at 350 ns. Other changes to the spectra include an appearance of another band's edge at ca. 450 nm and a growth of flat absorbance seen as vertical translation of the spectra after ca. 800 ns. Certainly the most striking feature in the spectra is the growth of a new absorption

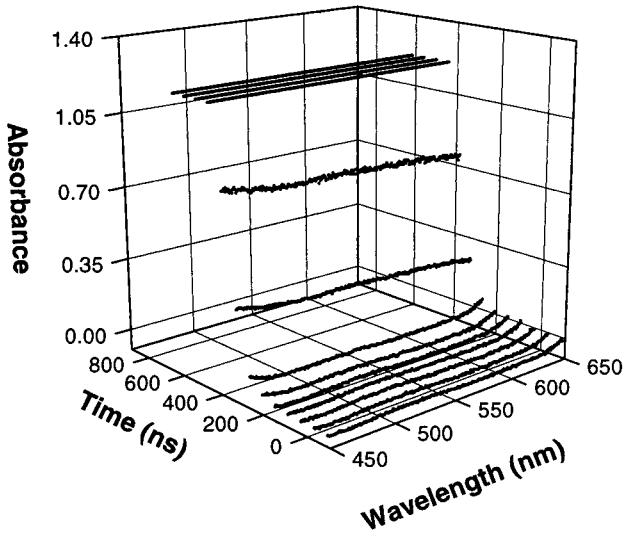

Figure 1. Time-resolved absorption spectra of neat NM shocked to 17.2 GPa (experiment A1). At 0 ns shock enters the sample; by 130 ns, the final pressure is reached. Sample was heated to 50 °C before experiment. Spectra were taken with 59 ns resolution. Last four spectra were acquired when the amount of light transmitted through the sample was below the dynamic range of the detection system.

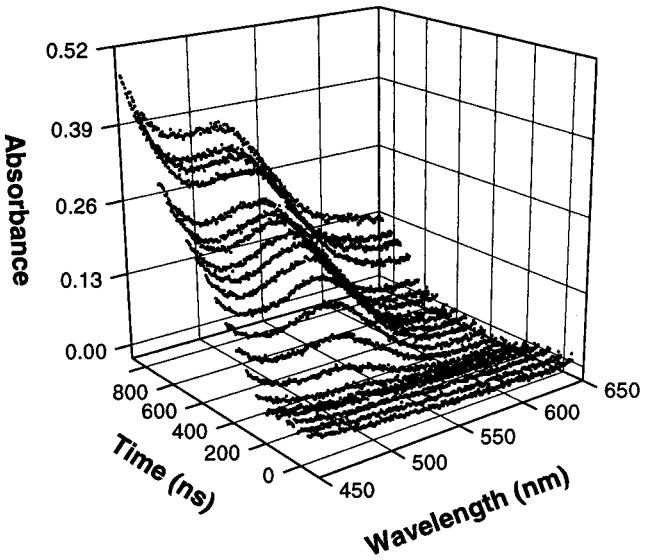

Figure 2. Time-resolved absorption spectra of NM + EDA (37.5 mM) mixture shocked to 12.1 GPa (experiment A2). At 0 ns shock enters the sample; by 350 ns, the final pressure is reached. Spectra were taken with 59 ns resolution.

band. We assign it to an intermediate formed in the NM−EDA mixture during early stages of decomposition. Flat absorbance is similar to that observed in neat NM (see experiment A1). Band edge appearance is consistent with results reported earlier.[7] The results of this experiment clearly indicate that the method used is sensitive to the initial chemical changes in sensitized NM. Moreover, it can be used to uncover the reaction mechanism since the intermediate can be identified eventually through its optical absorption spectrum.

Figure 3 shows a typical absorption spectrum of reacting NM−EDA mixture. To obtain the kinetics, we deconvoluted each spectrum into a sum of three components: a Gaussian, an exponential function, and a constant:

$$A(\lambda) = G \exp\left[-\left(\frac{\lambda - \lambda_0}{\Delta\lambda}\right)^2\right] + F \exp[-\alpha(\lambda - 430)] + C$$

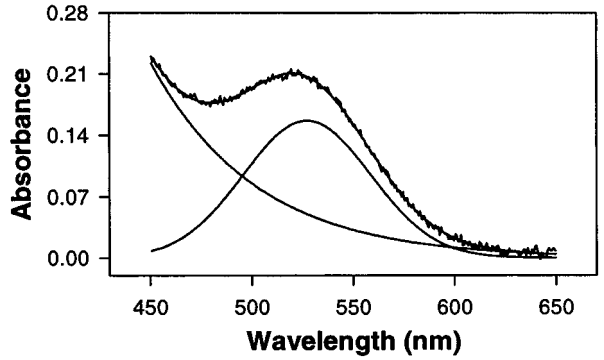

Figure 3. Absorption spectrum of NM + EDA (37.5 mM) mixture at 605 ns after the shock wave entered the sample (experiment A2). The spectrum is fitted to a sum of an exponential function, a Gaussian, and a constant. Smooth solid lines show the fit and its components.

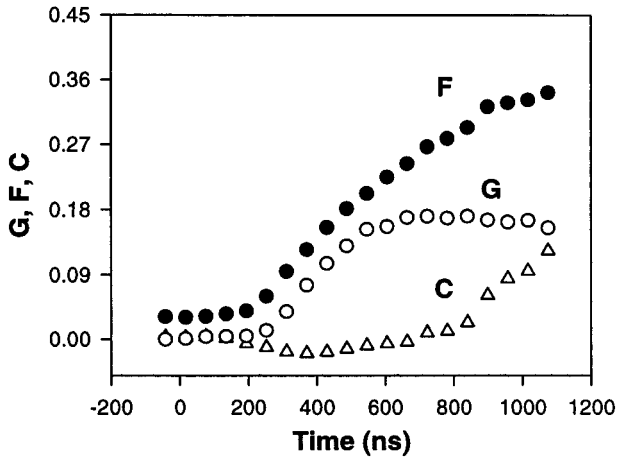

Figure 4. Kinetics of the components of the spectra of shocked NM + EDA (37.5 mM) mixture (experiment A2): *F*, preexponential factor; *G*, Gaussian peak height; *C*, constant.

where λ is wavelength in nanometers, G is the Gaussian peak height, λ_0 and $\Delta\lambda$ are the peak position and width, respectively, F is the preexponential factor, C is the constant, and α is the band edge constant. The three components represented the absorption band of the intermediate, the tail of a strong UV absorption band or combination of bands, and the flat absorbance, respectively. This particular function was chosen empirically to generalize the description of the absorption spectra in all 10 experiments (A1−A10) reported in this work. A representative least-squares fit is shown in Figure 3. The parameters of the fits i.e., *G*, *F*, and *C*, were taken as quantitative measures of the kinetics. It is important to note that, by definition, the value of *G* is proportional to the concentration of the intermediate. No such simple correspondence can be derived for either *F* or *C* values. Figure 4 shows the evolution in time of *G*, *F*, and *C* values in experiment A2. As can be seen, the kinetics of each is quite different. Therefore, it is reasonable to conclude that each one of them reflects concentration changes of different species. Below we will refer to the species contributing to *G*, *F*, and *C* values as G, F, and C species, respectively. Next, each component is discussed in more detail.

The results of experiments A2 and A3 (see also the next section) indicate that the G species exhibits steady-state kinetics: its concentration grows during transition time between 200 and 600 ns and then remains nearly constant through the end of experiment. Steady-state behavior implies a small extent of reaction since the reactants forming G must not be depleted by more than 10−30% by the end of experiment. Although there

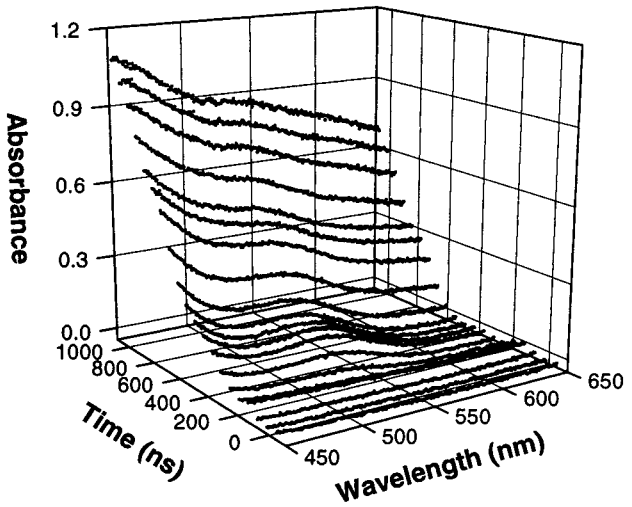

Figure 5. Time-resolved absorption spectra of NM + EDA (18.8 mM) mixture shocked to 14.0 GPa (experiment A3). At 0 ns shock enters the sample; by 315 ns, the final pressure is reached. Spectra were taken with 59 ns resolution.

is ca. 200 ns delay between the onset of G curve and the time when shock wave entered the sample, this corresponds to the temperature profile expected in this experiment. In other words, the intermediate G is formed in the first stage directly from reactant(s) present initially in NM−EDA mixture.

The onset of the F curve and its rise until ca. 500 ns are similar to those of the G curve. However, it continues to grow even after the G curve has leveled off. Although the interpretation of this kinetic behavior is not as straightforward as the previous one, it can be understood as follows: the *F* value is made up of at least two contributions. Before 350 ns its change is, at least partially, caused by the pressure increase in the sample. It could be a shifting tail from a shorter wavelength absorption band.[7] After 350 ns the growth of F is due to the products that begin to form in the decomposition process.

The *C* value describes flat featureless absorbance similar to that detected in experiment A1. Its timing is indicative of the products formed later than F and G. Its presence in both sensitized and neat NM experiments suggests that the reaction schemes likely converge at some point although the initial stages may be different.

C. Nitromethane−Ethylenediamine Mixture at 14 GPa. When sensitized NM is shocked to a pressure of 14 GPa, a greater extent of reaction is expected to be reached by 1 μs. In this subsection, we specifically examine the effects of higher pressure/temperature on the intermediates. Figure 5 shows a result of experiment A3 (see Table 1 for parameters). Although it differs quantitatively from experiment A2, it is qualitatively quite similar. All three components of the spectra seen in experiment A2 are clearly present in this experiment as well. To quantify them, we analyzed the spectra as presented in Figure 6.

As seen from the G curve in Figure 6, the concentration of the intermediate G goes through a maximum; it becomes very small by the end of experiment. This result clearly establishes that species G is indeed a transient intermediate, formed and then consumed, in the course of chemical reaction. It also justifies the interpretation of the G kinetics observed in experiment A2 (and then in experiments A4−A7, A9, and A10) as steady-state kinetics. The F and G curves, as expected, do not go through a maximum.

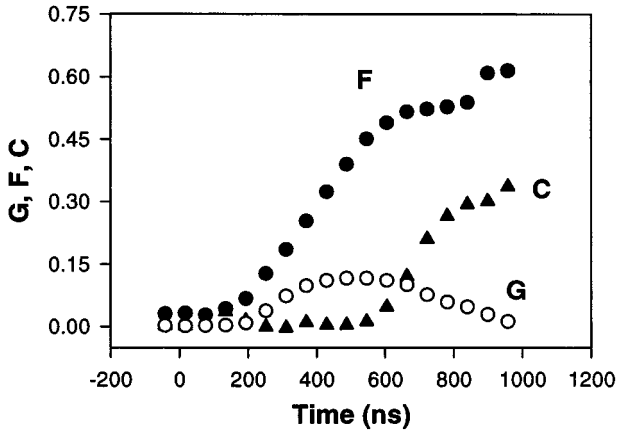

Figure 6. Kinetics of the components of the spectra of shocked NM + EDA (18.8 mM) mixture (experiment A3). The notation is the same as Figure 4.

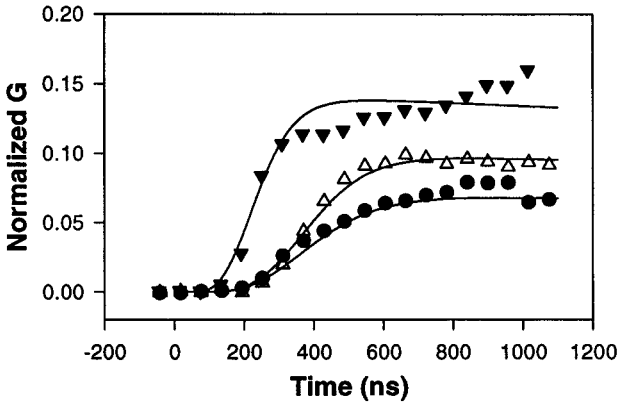

Figure 7. Gaussian peak height (*G*) normalized to the sample thickness of 160 μm versus time in experiments A2, A4, and A5. NM + EDA samples were shocked to about the same final pressure of 12 GPa. Different EDA concentrations were used: filled circles, 18.8 mM (experiment A4); open triangles, 37.5 mM (experiment A2); filled triangles, 75.0 mM (experiment A5). Solid lines represent the kinetic fits obtained as described in section VC.

D. Dependence on the Ethylenediamine Concentration. As summarized in section IIC, different authors have proposed different reactions as a first step in NM decomposition. These differences would imply different kinetics. As clearly indicated above, the G species is formed in the early stages of the reaction in sensitized NM. Thus, by monitoring the G species, one could directly probe the reaction kinetics. The dependence on the amine concentration would be instructive in this case.

Two experiments, A4 and A5 (see Table 1), were carried out at 12 GPa with EDA concentrations of 18.8 and 75.0 mM, respectively. The results of experiment A2 were also used to complete the set. Three-dimensional plots of the data looked very similar to that in Figure 2. Again, we analyzed them using the method described above. To compare the different results quantitatively, the kinetic curves were normalized to a cell thickness of 160 μm. The normalized *G* values obtained are plotted in Figure 7. In all three cases, nearly steady-state kinetics were observed. Different transition times were due to the different shock-up times (see Table 1). Least-squares fits of these data with the kinetic model described in section VC are shown in Figure 7 with the solid lines.

As mentioned above, the *G* value is proportional to the concentration of the intermediate formed. It is clearly seen from Figure 7 that the larger concentrations of the intermediate

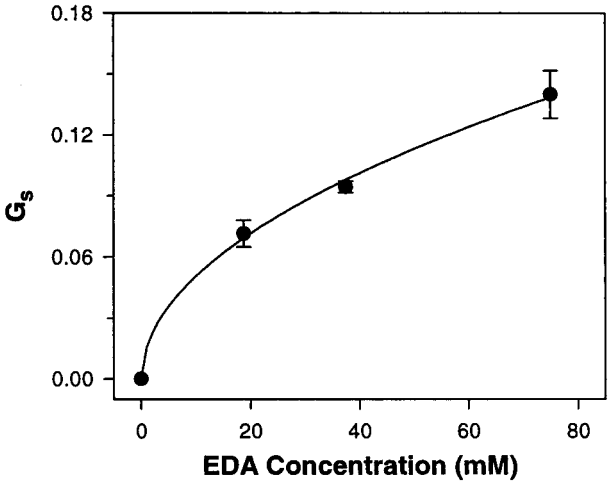

Figure 8. Average Gaussian peak height (G_s) as a function of EDA concentration in NM−EDA samples shocked to ca. 12 GPa (experiments A2, A4, and A5). Peak height is normalized to the sample thickness of 160 μm; averaging time is 600−1000 ns. Solid line represents the least-squares fit by eq 11.

correspond to the larger concentrations of EDA. The stationary G value, G_s, in turn, is a measure of the steady-state concentration of the intermediate. To obtain G_s, we averaged the points for each set of data over a 600−1000 ns time interval. The values obtained are plotted in Figure 8. The data were fitted well to the function $G_s \sim [\text{EDA}]^{1/2}$; the fit is shown in Figure 8 by the solid line. Further discussion of these results is postponed to section VC.

E. Nitromethane Sensitization by Primary, Secondary, and Tertiary Amines. In this section we describe the experimental results obtained using five different primary, secondary, tertiary, and di- amines. From these experiments we can examine how differences in chemical structure of the amines influence the reaction mechanism. This is useful both from an analytical viewpoint and in identification of the intermediate(s). To permit meaningful comparisons, we performed the experiments at comparable pressures and with the same amine concentrations. Various parameters for these experiments (A6−A10) are listed in Table 1.

In four of the experiments (A6, A7, A9, and A10), we obtained results that were very similar to each other and to the results for NM−EDA mixtures described in the preceding sections. A representative 3-dimensional plot, from experiment A9 with the NM−TEA mixture, is shown in Figure 9. The one experiment that gave different results was experiment A8 with the NM−MPA mixture. The data from this experiment are shown in Figure 10.

As seen from Figure 10, the peak at 525 nm did not develop in experiment A8. The UV band edge, however, appeared. Therefore, the only meaningful kinetic parameter that could be obtained from the analysis of these spectra was F. Its evolution in time, shown in Figure 11, correlates very well with the pressure profile in the sample. Thus, we conclude that the NM−MPA mixture has not started reacting within 1 μs at 12 GPa; i.e., MPA did not sensitize NM.

In all other experiments the mixtures reacted. The spectra at 600 ns after the shock wave entered the sample, for the five experiments, are compared in Figure 12. As clearly seen, the same peak at 525 nm developed in experiments A6, A7, A9, and A10. Moreover, the spectra look strikingly alike. Hence, we were able to analyze these four spectra, as described in section IVB, and the results are presented in Figure 13. All

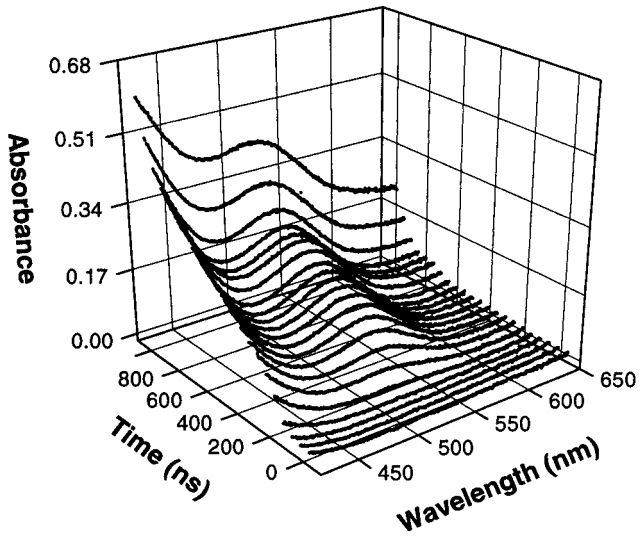

Figure 9. Time-resolved absorption spectra of NM + TEA (37.5 mM) mixture shocked to 11.8 GPa (experiment A9). At 0 ns shock enters the sample; by 210 ns, the final pressure is reached. Spectra were acquired with 49 ns resolution.

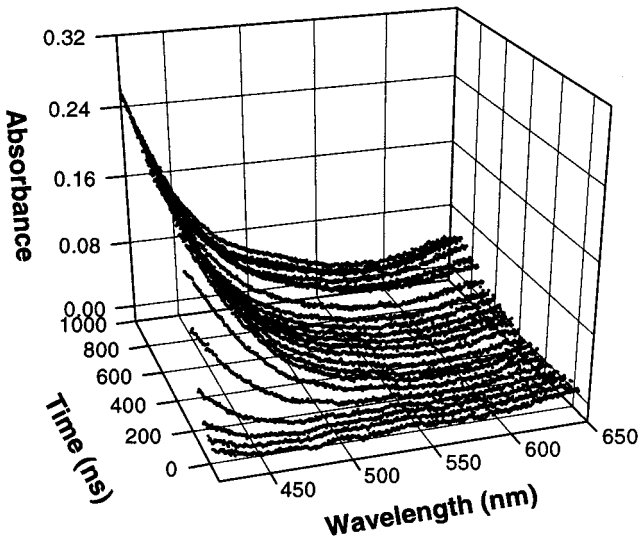

Figure 10. Time-resolved absorption spectra of NM + MPA (38.0 mM) mixture shocked to 11.8 GPa (experiment A8). At 0 ns shock enters the sample; by 195 ns, the final pressure is reached. Spectra were acquired with 49 ns resolution.

values shown were normalized to the standard sample thickness of 160 μm.

In all cases, steady-state kinetics were observed for intermediate G (Figure 13A). We obtained the stationary G values, G_s, by averaging the points for each set of data over the 600−1000 ns time interval. The results are shown in Table 2. The F kinetics are qualitatively similar in all cases (Figure 13B). There is a pressure-induced part before 200 ns, similar to that observed in experiment A8 (Figure 11). After 200 ns, F grows linearly in time through the end of the experiments. This can be interpreted as a steady rate of formation of the F species. It is difficult to attach much significance to the difference in slopes since the extinction coefficients are not known. The C kinetics are quite difficult to analyze (Figure 13C). They are presented primarily for completeness. Apparently, a larger extent of reaction occurred in the case of DEA.

The above results show that the same intermediate is formed in the course of shock-induced decomposition of NM sensitized by five different amines. This indicates that the same sensitiza-

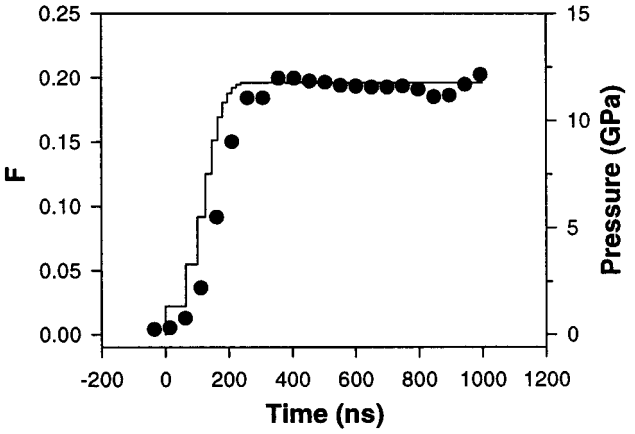

Figure 11. Variation with time of the *F* value (points) and the calculated pressure in the sample (line) for NM + MPA (38.0 mM) mixture shocked to 11.8 GPa (experiment A8).

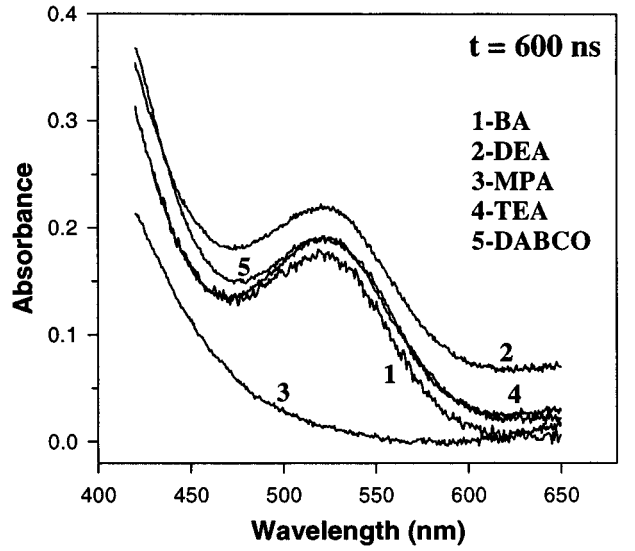

Figure 12. Absorption spectra of NM + amine mixtures at 600 ns after the shock wave entered the sample. The samples were shocked to ca. 12 GPa. Five different amines were used: (1) BA, experiment A6; (2) DEA, experiment A7; (3) MPA, experiment A8; (4) TEA, experiment A9; (5) DABCO, experiment A10.

tion mechanism is operative in all the NM−amine mixtures studied.

V. Analysis and Discussion

A. Intermediate Identification. Understanding the mechanism of amine sensitization of NM requires an identification of the intermediate (G). Therefore, we summarize the observations regarding the intermediate G: (a) it forms in shocked NM in the presence of various amines; (b) it has a characteristic band at 525 nm (with ca. 60 nm fwhm) in the optical absorption spectrum which does not depend on the particular amine used; (c) steady-state kinetics are observed at 12 GPa, and the steady-state concentration is approximately proportional to the square root of the amine concentration. Additionally, there is the general requirement of sensitization: it is easier for NM to decompose via the pathway that produces the intermediate G than via the pathway operative in neat NM.

The signature feature of intermediate G is the absorption band in the visible. Given the amine concentration used and the steady-state kinetics observed, we estimate the extinction coefficient of this band to be on the order of few thousand M^{-1} cm^{-1}. Such a value would be typical for an intramolecular dipole-allowed electronic transition.

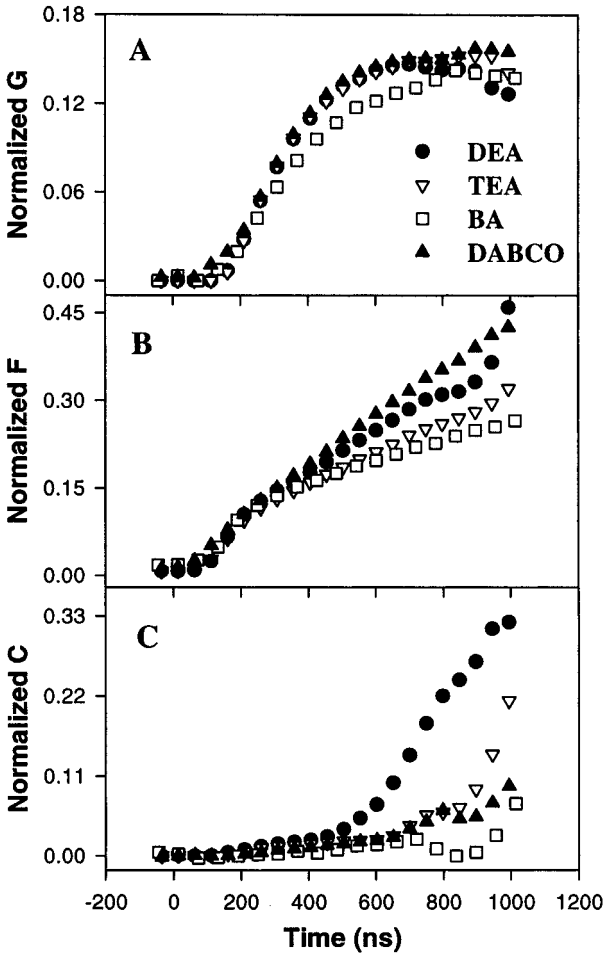

Figure 13. Kinetics of the components of the spectra of shocked NM + amine mixtures. The samples were shocked to ca. 12 GPa. Four different amines were used: BA, experiment A6, empty squares; DEA, experiment A7, filled circles; TEA, experiment A9, empty triangles; DABCO, experiment A10, filled triangles. (A) Gaussian peak height, *G*; (B) preexponential factor, *F*; (C) constant, *C*. All values are normalized to the sample thickness of 160 μm.

TABLE 2: G_s Values for Nitromethane−Amine Mixtures and pK_b Values of the Amines Used

amine	G_s	pK_b[a]
diethylamine	0.141 ± 0.007	3.07[23]
triethylamine	0.148 ± 0.004	3.13[23]
n-butylamine	0.135 ± 0.007	3.40[23]
ethylenediamine	0.094 ± 0.003[b]	3.94[23]
1,4-diazabicyclo[2.2.2]octane	0.152 ± 0.004	5.18[58]
N-methylaniline	0	9.15[59]

[a] pK_b values in water. [b] Experiment A2.

Although steady-state kinetics are often observed for radical intermediates, we sought to identify the intermediate among any plausible species. Among possible nonradical species that have bands in the visible, such as nitroso compounds, diazo compounds, etc., we have not found a molecule to match the above criteria. The analysis for radicals is more formidable because electronic absorption spectra of radicals are, in most cases, not readily available. It is generally expected that transitions by the unpaired electron between the energy levels of the radical require less energy than transitions of the paired electrons of the parent molecule.[38] A radical, therefore, tends to absorb light of longer wavelength than the fully bonded parent molecule,

and consequently many of the radicals are colored. Still, simple neutral radicals conceivably expected from NM or NM + amine did not seem to possess an absorption band as far into the visible as 525 nm. Another type of radical that tends to develop an absorption band of even longer wavelength than neutral radicals is radical ions. A radical anion of NM, $CH_3NO_2^{\bullet-}$, matched well the descriptions of intermediate G. Therefore, we tentatively assigned the intermediate to be $CH_3NO_2^{\bullet-}$. Below we discuss this assignment in more detail.

Radical anions of nitro compounds have long been known to form under electron impact in the gas phase, in electrochemical processes, and under radiolysis.[39−41] Some of them are known to be deeply colored[39,42] which implies the absorption band in the visible. To the best of our knowledge, we are unaware of published electronic absorption spectra of $CH_3NO_2^{\bullet-}$ radicals. Fortunately, some conclusions about the energy of the electronic transitions in these radicals can be formed from the data reported by Lobo et al.[43] They measured the energy loss spectra of potassium ions formed in collisions between potassium atoms and NM molecules:

$$K + CH_3NO_2 \rightarrow K^+ + CH_3NO_2^{\bullet-}$$

The typical spectrum consisted of two convoluted peaks: one at about 6.5 eV and the other at approximately 2 eV higher. The peaks constituted evidence for the presence of two electronic states in NM radical anion which were nearly 2 eV apart. The lower and upper peaks were identified as electron transfer from a potassium atom to the ground-state $CH_3NO_2^{\bullet-}$ ($^2A_1$) and to the excited states $CH_3NO_2^{\bullet-}$ ($^2B_1$), respectively.[43] Therefore, the energy difference between these two peaks should roughly correspond to the energy of electronic transition in the radical anion. It compares favorably with the energy of the band (2.36 eV) detected in our experiments and provides the first supporting point for the identification.

Furthermore, as follows from the electronic structure of the radical anion, it should fluoresce from the $^2B_1$ excited state.[43−46] We used this property to verify our identification independently in a separate set of experiments.[47] We did observe the expected fluorescence when the intermediate was excited with the 514 nm laser pulse. These experiments will be reported elsewhere.[47] Finally, the above identification is supported by the fact that the same intermediate was detected in different NM−amine mixtures because no amine specifics are involved in the radical anion formation.

It is generally accepted (see the background section) that cleavage of the C−N bond is a key step in the decomposition of NM.[4,9,18,29,30] Sensitization is likely to include a process that lowers the C−N bond dissociation energy in comparison to neat NM. From this point of view, the radical anion is an attractive pathway. Capture of an electron by NM elongates the C−N bond from 1.475 to 2.0 Å.[43,48] This subsequently lowers the dissociation energy from 245 kJ/mol ($CH_3 + NO_2$)[43,49] to around 50 kJ/mol ($CH_3 + NO_2^-$).[30,43] Therefore, the unimolecular decomposition of radical anions is expected to occur quite easily:

$$CH_3NO_2^{\bullet-} \rightarrow CH_3^{\bullet} + NO_2^- \qquad (6)$$

In addition, NM has a positive adiabatic electron affinity which is around 50 kJ/mol.[30,46] Hence, the radical anion is more favorable thermodynamically than the neutral molecule. This fact further strengthens the arguments in favor of the radical anion pathway. Below we analyze several possible radical anion mechanisms.

B. Reaction Mechanism. The simplest mechanism to form radical anions would be a direct electron transfer from the amine:

$$CH_3NO_2 + RNH_2 \rightarrow CH_3NO_2^{\bullet-} + RNH_2^{\bullet+} \qquad (7)$$

From the point of view of this reaction, an electron is most likely to be donated from the lone pair on the nitrogen atom of amine to a NM molecule. The efficiency of this process should be related to the ionization (or redox) potential of the donor and electron affinity of the acceptor. It is known that the ionization potential decreases by ca. 0.8 eV from primary to secondary and from secondary to tertiary amines.[50] Therefore, it would be expected that tertiary amines could serve as more effective donors. This, however, is not supported by our data which showed that all of the amines were approximately equally effective. Hence, we ruled out the direct electron transfer.

Another simple reaction, similar to reaction 7, might be a heterolytic dissociation of a NM−amine charge-transfer complex to produce a pair of radical ions:

$$[CH_3NO_2 \cdot\cdot RNH_2] \rightarrow CH_3NO_2^{\bullet-} + RNH_2^{\bullet+} \qquad (8)$$

The counterions formed here are aminium radicals. They are well-established transient intermediates;[51] they form in a great number of reactions including electron transfer from alkylamines, which is reaction 8. Therefore, the detection of aminium radicals could have conceivably been attempted in our experiments.

A significant body of spectral data is available for aminium radicals.[42,51−53] To permit detection in our experiments, a radical should possess a strong absorption band in the visible and be long-lived. The aminium radicals of DABCO and MPA seemed to meet these requirements. They have absorption bands around 460 nm.[42] The aminium radical of DABCO is also exceptionally long-lived among other aminium radicals because of the significant delocalization of the unpaired electron.[54−56] If either reaction 7 or 8 was responsible for generation of radical ions, we should have detected the absorption peaks corresponding to the aminium radical counterions in experiments A9 and A10. However, as seen in Figure 12, this did not happen in the case of DABCO; MPA did not sensitize NM at all. These results indicated that simple mechanisms such as electron transfer from amines or decomposition of charge-transfer complexes are not operative in NM−amine mixtures.

The result of experiment A9 contains an important piece of information if we can understand why MPA did not sensitize NM while all of the other amines did. The data presented in Table 2 suggest that the amine basicity is responsible for sensitization. Apparently, MPA did not sensitize NM because it is a noticeably weaker base than the rest of the amines used. In light of this observation, a plausible mechanism of sensitization would be the base catalysis by amines.

Several plausible base catalytic processes leading to the formation of radical anions may be proposed. One of them might be the following:

$$RNH_2 + 2CH_3NO_2 \rightarrow CH_3NO_2^{\bullet-} + CH_2NO_2^{\bullet} + RNH_3^+ \qquad (9)$$

This reaction is a bimolecular reaction between an amine molecule and an NM molecular dimer. Amine molecule acts here as a proton acceptor. The dimerization of NM is facilitated by the C−H···O hydrogen bonding in liquid NM[57] and effects of high pressure. Another plausible catalytic process might occur via the following two stages:

$$CH_3NO_2 + RNH_2 \rightleftharpoons [CH_2NO_2]^- + RNH_3^+ \quad (2)$$

$$[CH_2NO_2]^- + CH_3NO_2 \rightarrow CH_3NO_2^{\bullet -} + CH_2NO_2^{\bullet} \quad (10)$$

The first stage here is an acid−base equilibrium already discussed above to produce aci-anions and the protonated amine. In the second rate-determining stage, aci-anions react with NM to produce radical anions and nitromethyl radicals. Both catalytic mechanisms are likely to be followed by the decomposition of radical anions via reaction 6.

Unfortunately, none of the transient species in reactions 2, 6, 9, and 10 besides the radical anion can be detected with the spectral methods at our disposal. Hence, to further discriminate between possible mechanisms, we use a kinetic approach. The kinetic data are analyzed in the next section.

C. Reaction Kinetics. Given the results of Figures 7 and 8, we are in a position to be able to evaluate different kinetic schemes of reaction in sensitized NM. The nature of shock experiments, however, does not allow to collect a substantial amount of data. Hence, there might be a room for several kinetic models to fit the kinetic data satisfactory. On the other hand, the data are still conclusive enough to rule out quite a few possibilities. As an example, let us consider reaction 9. The kinetic scheme compiled for reactions 9 and 6 predicts that the steady-state concentration of radical anions will depend linearly on the amine concentration. However, this prediction contradicts the experimental data of Figure 8, and therefore, reaction 9 can be ruled out.

Several other kinetic schemes were analyzed in a similar fashion. The only scheme that produced a good fit to the kinetic data and, at the same time, was consistent physically and chemically was the one compiled of reactions 2, 6, and 10:

$$CH_3NO_2 + RNH_2 \rightleftharpoons [CH_2NO_2]^- + RNH_3^+ \quad (2)$$

$$[CH_2NO_2]^- + CH_3NO_2 \rightarrow CH_3NO_2^{\bullet -} + CH_2NO_2^{\bullet} \quad (10)$$

$$CH_3NO_2^{\bullet -} \rightarrow CH_3^{\bullet} + NO_2^- \quad (6)$$

If reaction 10 is the rate-limiting stage here, the steady-state concentration, $[CH_3NO_2^{\bullet -}]_s$, can be easily derived as

$$[CH_3NO_2^{\bullet -}]_s = (k_{10}/k_6)\sqrt{K_2}[CH_3NO_2]^{3/2}\sqrt{[RNH_2]} \quad (11)$$

where K_2 is the equilibrium constant, k_{10} and k_6 are the rate constants of reactions 10 and 6, respectively, and $[CH_3NO_2]$ and $[RNH_2]$ are the concentrations of NM and amine. Least-squares fit of the experimental data by eq 11 is shown by the solid line in Figure 8. As can be seen, the scheme could fit well the data of Figure 8. It is interesting to note that this mechanism predicts also the similar square root dependence on the amine concentration for the reciprocal failure diameter. In fact, this agrees very well with the failure diameter measurements of Engelke[13] where he found this relationship empirically.

We attempted to further evaluate this kinetic scheme by testing its ability to model the data of Figure 7 over the entire 1 μs range. It was done in three steps. First, we obtained the temperature profile in the sample by running the SHOCKUP code[34] and averaging the temperature over the sample thickness. We assumed the temperature to be constant after the shock-up time through the end of experiment. Three different temperature profiles were calculated for experiments A2, A4, and A5. Second, we used these temperature profiles to solve numerically the differential equations describing the reaction scheme. Besides the difference in temperature profiles, there is just one parameter changing in this series, i.e., [EDA]. Therefore, we incorporated it into the algorithm and fitted all three sets of data *simultaneously* with a single set of parameters. The algorithm was run to minimize a sum of weighted square deviations taken over entire data. A representative fit is shown in Figure 7 by solid lines. As can be seen, both transient and steady parts of the kinetics are modeled well with the scheme. The fitting procedure yielded the activation energy of the rate-limiting step to be ca. 70 kJ/mol with an estimated standard deviation of ±20 kJ/mol.

Combining together all the experimental evidence and analyses presented above, we conclude that the mechanism composed of reactions 2, 10, and 6 describes best the decomposition process in sensitized NM.

VI. Concluding Remarks

The mechanism of amine sensitization of shocked nitromethane was investigated using time-resolved optical absorption spectroscopy in the visible. Nitromethane−amine mixtures react via formation of an intermediate that gives rise to a transient absorption peak at 525 nm. The same intermediate is detected for nitromethane mixtures with five different primary, secondary, and tertiary amines. At 12 GPa and 730 K the steady-state kinetics are observed with the intermediate concentration proportional to the square root of amine concentration. On the basis of our analysis and the data available from the literature, we identify the intermediate as radical anion of nitromethane, $CH_3NO_2^{\bullet -}$. Possible reaction mechanisms are discussed and evaluated. Among the several considered, the following mechanism is favored:

$$CH_3NO_2 + RNH_2 \rightleftharpoons [CH_2NO_2]^- + RNH_3^+$$

$$[CH_2NO_2]^- + CH_3NO_2 \rightarrow CH_3NO_2^{\bullet -} + CH_2NO_2^{\bullet}$$

$$CH_3NO_2^{\bullet -} \rightarrow CH_3^{\bullet} + NO_2^-$$

The sensitization of NM is brought about by the significantly lower C−N bond dissociation energy in the radical anion than in the neutral molecule of NM. The radicals formed as products in the processes of formation and decomposition of radical anions will sustain reaction by starting out chain reactions of bulk NM decomposition.

Among the mechanisms proposed earlier,[18,29,30] none can account for the experimental observations presented in this work. The aci-anion hypothesis of Engelke et al.,[13,14,25−27] stating that the aci-anion of nitromethane is involved in the unspecified rate-limiting step of the decomposition process, is consistent with the mechanism shown above. Hence, the experimental results that led to that hypothesis can be considered as an additional piece of evidence in support of the mechanism proposed.

Acknowledgment. D. Savage and K. Zimmerman are thanked for their assistance in the experimental effort. Discussions with Dr. J. M. Winey and Dr. G. I. Pangilinan are gratefully acknowledged. This work was supported by ONR Grant N00014-93-1-0369.

References and Notes

(1) Cheret, R. *Detonation of Condensed Explosives*; Springer-Verlag: New York, 1993.

(2) Gupta, Y. M. *J. Phys. IV, Colloq. C4* **1995**, *5*, C4-345.

(3) Winey, J. M. Time-resolved optical spectroscopy to examine shock-induced decomposition in liquid nitromethane. Ph.D. Dissertation, Washington State University, 1995.
(4) Constantinou, C. P. The nitromethane-amine interaction. Ph.D. Dissertation, Cambridge University, 1992.
(5) Piermarini, G. J.; Block, S.; Miller, P. J. *J. Phys. Chem*. **1989**, *93*, 457.
(6) Hardesty, D. R. *Combust. Flame* **1976**, *27*, 229.
(7) Constantinou, C. P.; Winey, J. M.; Gupta, Y. M. *J. Phys. Chem*. **1994**, *98*, 7767.
(8) Pangilinan, G. I.; Gupta, Y. M. *J. Phys. Chem*. **1994**, *98*, 4522.
(9) Gupta, Y. M.; Pangilinan, G. I.; Winey, J. M.; Constantinou, C. P. *Chem. Phys. Lett.* **1995**, *232*, 341.
(10) Winey, J. M.; Gupta, Y. M. *J. Phys. Chem. A* **1997**, *101*, 9333.
(11) Winey, J. M.; Gupta, Y. M. *J. Phys. Chem. B* **1997**, *101*, 10733.
(12) Eyster, E. H.; Smith, L. C.; Walton, S. R. US Naval Ordnance Lab. Report No. NOLM 10336, 1949.
(13) Engelke, R. *Phys. Fluids* **1980**, *23*, 875.
(14) Engelke, R.; Earl, W. L.; Rohlfing, C. M. *J. Chem. Phys*. **1986**, *84*, 142.
(15) Cook, M. D.; Haskins, P. J. In *Proceedings of the 19th International Annual Conference of ICT on Combustion and Detonation Phenomena*; Karlsruhe, Germany; Fraunhofer Institut fur Chemische, Technologie, Explosivstoffe: Karlsruhe, Germany, 1988; p 85-1.
(16) Forshey, D. R.; Cooper, J. C.; Doyak, W. J. *Explosivstoffe Nr*. **1969**, *6*, 125.
(17) Kondrikov, B. N.; Kozak, G. D.; Raikova, V. M.; Starshinov, A. V. *Dokl. Akad. Nauk SSSR* **1977**, *233*, 402.
(18) Constantinou, C. P.; Mukundan, T.; Chaudhri, M. M. *Philos. Trans. R. Soc. London A* **1992**, *339*, 403.
(19) Bhujle, V. V.; Randhawa, H. S. *Indian J. Chem*. **1972**, *10*, 945.
(20) McEwen, K. L. *J. Chem. Phys*. **1960**, *32*, 1801.
(21) Rao, C. N. R. In *The Chemistry of the Nitro and Nitroso Groups*; Feuer, H., Ed.; Wiley: New York, 1969; Part 1, p 92.
(22) Foster, R. *Organic Charge-Transfer Complexes*; Academic Press: New York, 1969.
(23) Rabinovich, V. A.; Havin, Z. Y. *Brief Chemical Handbook*; Khimiya: Leningrad, 1978.
(24) King, E. J. In *Physical Chemistry of Organic Solvent Systems*; Covington, A. K., Dickinson, T., Eds.; Plenum Press: New York, 1973; p 331.
(25) Engelke, R.; Schiferl, D.; Storm, C. B.; Earl, W. L. *J. Phys. Chem*. **1988**, *92*, 6815.
(26) Engelke, R.; Earl, W. L.; Rohlfing, C. M. *Int. J. Chem. Kinet*. **1986**, *18*, 1205.
(27) Engelke, R.; Earl, W. L.; Rohlfing, C. M. *J. Phys. Chem*. **1986**, *90*, 545.
(28) Miller P. J.; Block, S.; Piermarini, G. J. *J. Phys. Chem*. **1989**, *93*, 462.
(29) Cook, M. D.; Haskins, P. J. *Proc. 9th Symp. (Int.) Detonation* **1989**, 1027; *Proc. 10th Symp. (Int.) Detonation* **1993**, 870.
(30) Politzer, P.; Seminario, J. M.; Zacarias, A. G. *Mol. Phys.* **1996**, *89*, 1511.
(31) Yoo, C. S.; Duvall, G. E.; Furrer, J.; Granholm, R. *J. Phys. Chem*. **1989**, *93*, 3012.
(32) Fowles, G. R.; Duvall, G. E.; Asay, J.; Bellamy, P.; Feistman, F.; Grady, D.; Michaels, T.; Mitchell, R. *Rev. Sci. Instrum*. **1970**, *41*, 984.
(33) Ogilvie, K. M.; Duvall, G. E. *J. Chem. Phys*. **1983**, *78*, 1077.
(34) Ogilvie, K. M.; Duvall, G. E.; Collins, R. SHOCKUP Computer Code, Washington State University, Shock Dynamics Center, 1984.
(35) Barker, L. M.; Hollenbach, R. E. *J. Appl. Phys.* **1970**, *41*, 4208.
(36) Carter, W. J. *High Temp.*−*High Pressures* **1973**, *5*, 313.
(37) Winey, J. M.; Knudson, M. D.; Duvall, G. E.; Gupta, Y. M. Manuscript in preparation.
(38) Nonhebel, D. C.; Walton, J. C. *Free Radical Chemistry*; Cambridge University Press: New York, 1974.
(39) Greenstock, C. L. In *The Chemistry of Amino, Nitroso and Nitro Compounds and Their Derivatives*; Patai, S., Ed.; Wiley: New York, 1982; Suppl. F, Part 1, p 291.
(40) Russel, G. A.; Norris, R. K. In *Organic Reactive Intermediates*; McManus, S. P., Ed.; Academic Press: New York, 1973; p 423.
(41) Fry, A. J. In *The Chemistry of Amino, Nitroso and Nitro Compounds and Their Derivatives*; Patai, S., Ed.; Wiley: New York, 1982; Suppl. F, Part 1, p 319.
(42) Shida, T. *Electronic Absorption Spectra of Radical Ions*. Elsevier: Amsterdam, 1988.
(43) Lobo, R. F. M.; Moutinho, A. M. C.; Lacmann, K.; Los, J. *J. Chem. Phys*. **1991**, *95*, 166.
(44) Kimura, M.; Lacmann, K. *Chem. Phys. Lett.* **1980**, *70*, 41.
(45) Trawick, W. G.; Eberhardt, W. H. *J. Chem. Phys*. **1954**, *22*, 1462.
(46) Compton, R. N.; Reinhardt, P. W.; Cooper, C. D. *J. Chem. Phys*. **1978**, *68*, 4360.
(47) Gruzdkov, Y. A.; Gupta, Y. M. *J. Phys. Chem. A*, in press.
(48) Ramondo, F. *Can. J. Chem*. **1992**, *70*, 314.
(49) Sehon, R.; Szware, G. *Annu. Rev. Phys. Chem*. **1957**, *8*, 439.
(50) Aue, D. H.; Webb, H. M.; Bowers, M. T. *J. Am. Chem. Soc*. **1976**, *98*, 311.
(51) Chow, Y. L.; Danen, W. C.; Nelsen, S. F.; Rosenblatt, D. H. *Chem. Rev*. **1978**, *78*, 243.
(52) Goez, M.; Sartorius, I. *J. Am. Chem. Soc*. **1993**, *115*, 11123.
(53) Wagner, B. D.; Ruel, G.; Lusztyk, J. *J. Am. Chem. Soc*. **1996**, *118*, 13.
(54) Eastland, G. W.; Symons, M. C. R. *Chem. Phys. Lett.* **1977**, *45*, 422.
(55) McKinney, T. M.; Geske, D. H. *J. Am. Chem. Soc*. **1965**, *87*, 3013.
(56) Malatesta, V.; Ingold, K. U. *J. Am. Chem. Soc*. **1973**, *95*, 6400.
(57) Seminario, J. M.; Concha, M. C.; Politzer, P. *J. Chem. Phys*. **1995**, *102*, 8281.
(58) Staley, R. H.; Beauchamp, J. L. *J. Am. Chem. Soc*. **1974**, *96*, 1604.
(59) Smith, J. W. In *The Chemistry of the Amino Group*; Patai, S., Ed.; Wiley: New York, 1968; p 161.